

# Preliminary Magnitude and Distance Damage Thresholds for Light-Frame Wood Buildings in Induced Earthquakes

Bridger W. Baird

*Graduate Student, Dept. of Civil Engineering, University of Colorado, Boulder, USA*

Abbie B. Liel, Ph.D.

*Associate Professor, Dept. of Civil Engineering, University of Colorado, Boulder, USA*

Robert E. Chase, Ph.D.

*Associate, Exponent, Denver, USA*

**ABSTRACT:** Since 2009, the frequency of (moment) magnitude ( $M_w$ ) 3.0 earthquakes and larger in the Central United States, and especially Oklahoma (OK), has risen from an average of 2 per year, to 200-700 per year. This increase in seismicity is a result of injection of large quantities of wastewater generated from oil and gas activities deep underground. In this study, damage to built infrastructure from induced earthquakes is investigated through nonlinear dynamic analysis and probabilistic damage assessment for a light-frame wood structure. Specifically, we focus here on investigating the smallest  $M_w$  injection-induced earthquake that may cause damage to the building of interest at various distances from the hypocenter ( $R$ ). The simulations are based on a two-story multifamily dwelling, which is designed with lateral strength and detailing consistent with modern code requirements in Pawnee, OK. For a  $M_w$  4.5 earthquake, damage is observed at  $R = 15$  km or closer. While for an earthquake  $R = 3$  km from the site, damage is observed 56% of the time at  $M_w$  4.5 and occurs 100% of the time when  $M_w$  5.5 and above.

## 1. INTRODUCTION

Small to moderate (moment) magnitude ( $M_w$ ) shallow earthquakes have the potential to cause significant damage to buildings and infrastructure, and, in some cases, may even threaten life safety. For example, on August 21<sup>st</sup>, 2017, a relatively small earthquake ( $M_w$  3.9) struck the island of Ischia, Italy. The earthquake caused extensive localized damage and resulted in 2 deaths, 42 injuries, and the displacement of 1,000 people (Briseghella et al. 2018). The significance of the damage was attributed to the earthquake's shallow focal depth of 1.7 km, the unconsolidated soil on the island, and the vulnerability of the unreinforced masonry building stock (Briseghella et al. 2018).

The U.S. state of Oklahoma (OK) and nearby states have experienced a large number of shallow, small to moderate magnitude, earthquakes in recent years. Between 2009 and 2015 the frequency of  $M_w$  3.0 earthquakes and larger in OK rose from an average of 2 per year, to over 700 per year; 2017 earthquake rates were about 300 per year, and 2018 earthquake rates

were about 190 per year (OK Geologic Survey 2018). This elevated seismicity is the result of the injection of large quantities of wastewater from oil and gas production deep underground (Weingarten et al. 2015). These induced earthquakes have resulted in an associated increase in seismic hazard (Petersen et al. 2018), and correspondingly, an increase in the risk to infrastructure and buildings in OK and southern Kansas (Liu et al. 2019). The increase in seismic activity is of particular concern due to the region's building stock, much of which lacks seismic detailing, and evidence that the small to moderate magnitude events experienced to date can cause damage and economic impacts. Damage observed in the 2016  $M_w$  5.0 Cushing, OK earthquake included cracking in mortar joints, spalling of brick veneer, racking of structures, broken utility lines, damage to brick chimneys, etc. (Barba-Sevilla et al. 2018).

This paper examines the relationship between earthquake characteristics, particularly magnitude and hypocentral distance from the

source to the site ( $R$ ), and the resulting damage, focusing on injection-induced earthquakes and construction patterns of the central U.S. Our goal is to identify those magnitude and distance combinations that may cause damage (i.e. cracking to gypsum wallboard) to buildings. Smaller magnitude events, and their potential to cause damage, have not been much studied by earthquake engineers.

## 2. OVERVIEW OF METHODS

To investigate magnitude and distance thresholds for damage, we examine scenarios of magnitude and distance that could damage the typical building stock in OK. These scenarios are defined in Table 1. Scenario Set 1 corresponds to a  $M_w$  4.5 event, occurring at distance  $R$  of 3-35 km from a building of interest. For Scenario Set 1, a  $M_w$  4.5 event was selected because it represents the median  $M_w$  of the induced events that produced ground motions used in this study (see Figure 1) (Assatourians et al. 2017) and is a typical magnitude for the larger of the recently experienced injection-induced earthquakes. Scenario Set 2 is an event with a  $R$  of 3 km, with  $M_w$  3 to 6. For Scenario Set 2, a  $R$  of 3 km was selected because it is assumed to be the smallest possible  $R$  distance between an induced event and a structure.

This study makes use of recorded ground motions from induced earthquakes in OK and Alberta, CA for dynamic analysis. These ground motions are obtained from the Assatourians et al. (2017) database, which is a compilation of 68 3-component sets of ground motions. For this study, we are considering both horizontal components of the ground motions. This study excludes the vertical component of acceleration from the dynamic analysis.

Light-frame wood structures are the primary building type in OK and elsewhere in the U.S., and a two-story building archetype is analyzed to be representative of the typical new multifamily building stock in the OK region. The building is modeled using Timber3D, which is a nonlinear structural analysis software for wood frame buildings based in MATLAB that was developed by Pang and Hassanzadeh (2013).

Table 1: Earthquake scenarios considered in this study in terms of  $M_w$  and  $R$ .

Scenario Set 1 ( $M_w = 4.5$ )								
$R$ (km)								
3	5	7.5	10	15	20	25	30	35

Scenario Set 2 ( $R = 3$ km)						
$M_w$						
3	3.5	4	4.5	5	5.5	6

The building models are subjected to induced ground motions scaled to match the Scenario Sets, and the responses recorded. The engineering demand parameter we are considering is the maximum story drift ratio (MDR), defined as the largest drift occurring in either story. We define the first occurrence of damage for light wood frame structures consistent with FEMA P-58 as 0.2% MDR (FEMA 2012). The first occurrence of damage consists of gypsum wallboard cracking, screws popping out, and warping or cracking of plaster or paint finishes.

## 3. GROUND MOTION SELECTION AND SCALING

### 3.1. Earthquake Scenario Target Spectrum

Our goal is to analyze a structure subjected to a postulated scenario of engineering interest, such as  $M_w$  4.5 with  $R$  of 10 km. To do so, it is necessary to select and scale records to match the appropriate intensities and frequency content of the scenario, which may be significantly different from the scenarios producing the as-recorded motions. In order to determine the appropriate intensities, we use a ground motion prediction equation (GMPE) that was developed specifically for induced earthquake in OK, which we refer to as NAA-18 (Novakovic et al. 2018). This GMPE takes as input structural period, hypocentral distance, magnitude, rupture depth, and  $V_{S30}$  (which is the average shear wave velocity over the top 30 km of the site) and produces probabilistic estimates of peak ground acceleration and spectral accelerations.

The NAA-18 GMPE is a region-specific GMPE that was developed using a processed database of approximately 7,300 ground motion recordings from OK, the majority of which are considered to be induced by wastewater injection (Novakovic et al. 2018). The NAA-18 GMPE uses the framework of another GMPE produced by Yenir and Atkinson (2015) (YA-15), which was previously identified as being applicable to induced events (Atkinson and Assatourians 2017). The generic YA-15 GMPE was calibrated and turned into the NAA-18 GMPE by determining an anelastic attenuation function, OK-specific amplification models, regional stress parameters, and a calibration factor for the 7,300 induced OK ground motions.

An example of the target response spectra for one of our scenarios is shown in Figure 2.

### 3.2. Ground Motion Selection and Scaling

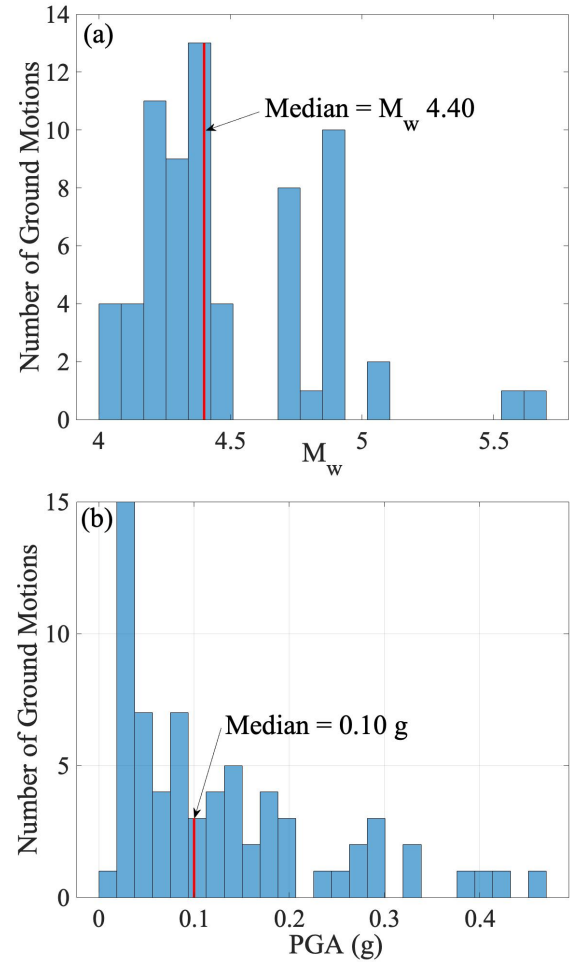
The ground motions used for these study are recorded between 2010 to 2016, with  $M_w$  larger than 4.0, and  $R$  less than 50 km (Assatourians et al. 2017). A summary of the ground motion characteristics for all records included in the database is shown in Figure 1.

Here, we adopt a ground motion selection algorithm developed by Baker and Lee (2018). The selection algorithm selects motions that have the mean and standard deviation consistent with a target response spectra. Our target spectra is produced from the NAA-18 GMPE. The NAA-18 GMPE provides the logarithmic mean and standard deviation of spectral acceleration at a range of periods.

The procedure for the selection algorithm, modified from Baker and Lee (2018), are: (1) compute a target median and standard deviation in response spectra using the NAA-18 GMPE, (2) statistically simulate response spectra to match the target spectral response distribution, (3) load and screen the induced record database from Assatourians et al. (2017), (4) select and scale the induced motion sets to match each of the statistically simulated spectra, and (5) make incremental changes to the initially selected induced motions and scale factors to improve the match with the target distribution. The scale

factors are selected to minimize the deviation of the selected record from the target spectra.

The output of the selection algorithm for a given scenario magnitude and distance combination are the selected two-motion sets, and the appropriate linear scaling factors. We applied no minimum or maximum limit to the scale factors for the records.



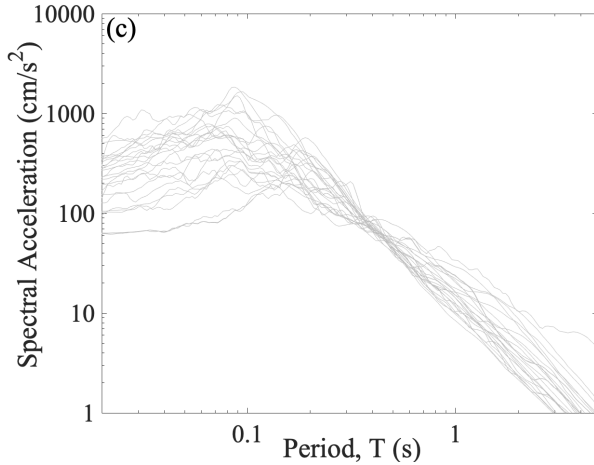


Figure 1: Ground motion characteristics for all 68 induced motions collected showing (a) earthquake  $M_w$ , (b) geomean PGA, and (c) as recorded geomean acceleration response spectra.

In order to quantify the structural response, and the statistical variation of the response, enough ground motions were required to simulate dynamic analysis for a given scenario. There are a number of different guidelines for the number of motions that should be run. For example, design standards, like the ASCE 7 document, require 7 to 11 records to demonstrate design adequacy (ASCE 2016). However, a study conducted by Kiani et al. (2018) analyzing the number of required simulations suggests that at least 25 hazard consistent ground motions are required to accurately and reliably estimate the collapse fragility curves. Baker (2018) suggests that 25-40 motions should be sufficient to get a quantify variability in response. For these reasons, we ran 25 ground motions for each scenario of interest.

The result of the 25 selected records using the described modification of Baker and Lee's (2018) selection algorithm for a  $M_w$  4.5 and  $R$  of 7.5 km event is shown in Figure 2.

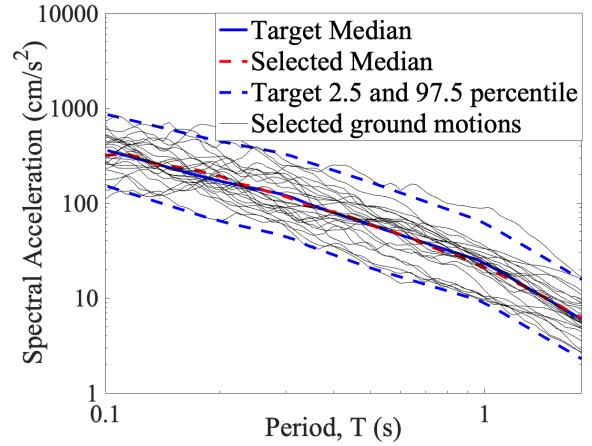


Figure 2: Selected and scaled ground motion records showing the target median, the median of the 25 selected records, and the target spread for a  $M_w$  4.5 and  $R$  of 7.5 km event.

#### 4. BUILDING ARCHETYPE

##### 4.1. Building Design

The two-story multifamily building considered in this study was originally designed for “moderate seismicity” according to ASCE 7-16 (ASCE 2017) by the ATC 116 project team. In that context, “moderate seismicity” refers to the upper limits of seismic design category (SDC) C, which has a short period response acceleration parameter ( $S_{DS}$ ) of 0.50g (ASCE 2017). OK is in SDC B. As a result, the buildings were redesigned for a location in Pawnee, OK with  $S_{DS}$  of 0.139g using the same wall layouts as the original models. In order to reduce the lateral strength of the original building design, the shear wall lengths were reduced, smaller nails were used, and the nail spacing was increased. We confirmed that the SDC B seismic forces were the controlling lateral design force when compared with wind.

The footprint of the two-story multifamily building is 14.6 m by 29.3 m and includes four adjacent two-story 7.31 m by 14.6 m townhouses. See Figure 3 for a floorplan of the building. The exterior walls are framed with 3.8x14.4 cm lumber, and have oriented strand board (OSB) sheathing, and are clad in exterior James Hardie fiber cement siding, which is a common siding type in OK. The selection in exterior finishes is important because the finishes can have a

substantial impact on the seismic response (Filiatrault et al. 2002). We discuss later how the exterior finishes is included in the nonlinear response of the structure. The interior face of the exterior walls is clad with 12.7 mm gypsum wallboard, and the interior shear walls are one line of 3.8x8.9 cm framing separated by a 2.5 cm gap. The foundation for the building is a 10 cm concrete slab on grade, with spread footings at the interior posts and reinforced grade beams integrated into the slab at the perimeter, and along the load bearing walls. The floor system is framed with 3.8x8.9 cm parallel chord trusses, spaced at 61 cm on center. More detailed descriptions of the building design are provided in (Chase 2018).

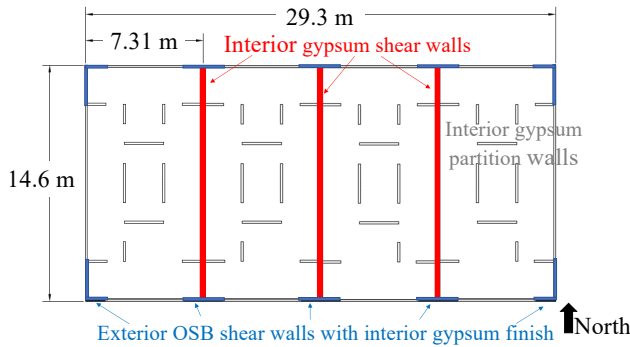


Figure 3: Floorplan of the two-story multifamily building.

#### 4.2. Building Modeling

The building is modeled using Timber3D, a software intended for simulating seismic response of 3D light-frame wood buildings, which aims to capture individual wood frame elements and the interaction of their responses up to large horizontal and vertical displacements. The model used is adapted from models from ATC 116, which were provided by Ghehnavjeh (2017).

Nonlinear behavior is modeled only in the wall elements. For this model, the nonlinear components are the interior and exterior shear walls, and the James Hardie fiber cement type siding on the exterior shear walls. The interior shear walls form the partition walls between units. The shear walls are the sole lateral force resisting system in the building. For the exterior walls, the

nonlinear response sums the hysteretic properties from the exterior OSB shear walls and the exterior siding. Figure 4 shows the hysteretic properties of all nonlinear elements considered in the two-story multifamily building.

The concrete foundation, sill plates, stud elements, and floor diaphragms are modeled as elastic elements, while the hold downs, anchor bolts, and soil elements are all modeled to be rigid. The diaphragms are modeled to be elastic, but very stiff, which is consistent with ATC 116. The base of the structure is modeled with multiple elements to simulate the effects of hold downs, anchor bolts, sill plates, the concrete foundation, and even the surrounding soil, which results in an effectively fixed base.

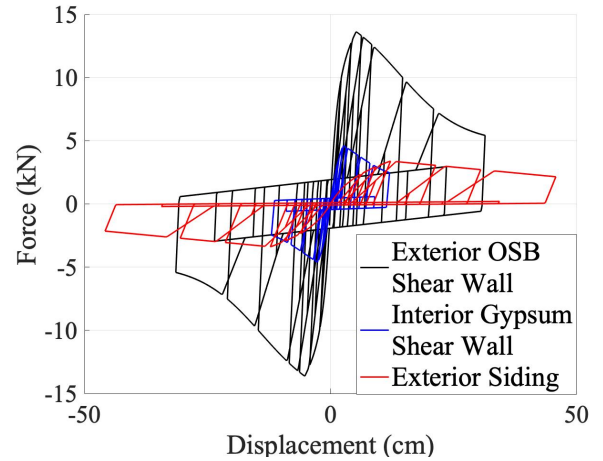


Figure 4: Hysteretic properties for Timber3D non-linear wall elements. The hysteretic properties are for 1.2 m by 2.4 m wall elements. The exterior siding is James Hardie fiber cement type siding.

In accordance with other previous studies (Pang and Shirazi 2013), we applied 1% Rayleigh damping to the first and second modes (E-W and N-S lateral directions) of the building. This damping is applied to represent linear elastic damping. Raleigh damping of 1% was selected to avoid overdamping in the nonlinear range.

The fundamental period of the two-story multifamily archetype is  $T_1 = 0.45$  s. Pushover curves for the multifamily building are shown in Figure 5.



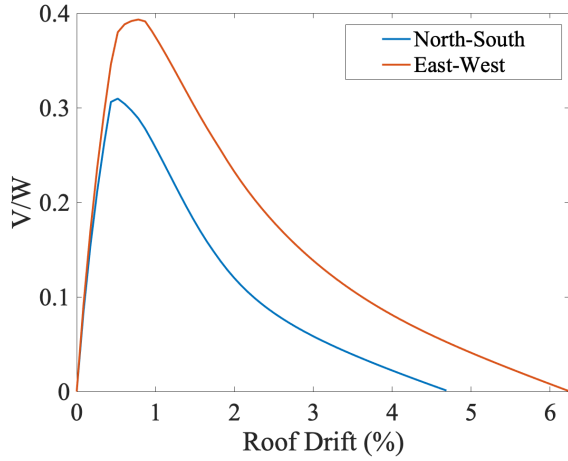


Figure 5: Pushover curves for the multifamily building.  $V/W$  is the base shear normalized by the building weight.

## 5. DAMAGE ASSESSMENT METHOD

The damage state of interest corresponds to 0.2% MDR. This threshold is associated with minor damage to structural shear wall and nonstructural wall elements, including screws popping out and minor cracking of gypsum wallboard. This threshold likely corresponds to the first damage in this kind of building that will require repairs (FEMA 2012).

We then post-process the Timber3D outputs to determine whether or not damage was reached. The results provide the probability of damage given a particular magnitude and distance scenario.

## 6. RESULTS

Figure 6 and Figure 7 shows the MDR results for Scenario Sets 1 and 2, and the probability of buildings reaching the damage state, respectively. For Scenario Set 1, as the  $M_w$  4.5 event gets closer to the building, the drift increases, which is to be expected. The variability among the drifts also increases as the earthquake gets closer to the building due to larger record to record variability and variability due to nonlinear response in more intense motions. None of the ground motions produce drift consistent with our damage threshold from Scenario 1, until the earthquake is at  $R$  of 15 km where the damage occurs in 4% of the ground motions. Figure 8 shows the geographical extent of damage for Scenario Set 1.

A  $M_w$  4.5 has the potential to cause damage at  $R$  up to 15 km. The highest probability of damage for Scenario Set 1 is  $R$  of 3 km, where the fraction of building damage dramatically increases to 56% of the earthquakes.

For Scenario Set 2, as the magnitude increases for a fixed  $R$  of 3 km the drift increases, again as expected. Similar to Scenario Set 1, the variability in drift increases as the earthquake magnitude gets higher as a result of the increased record to record variability and nonlinear response. No damage is observed for Scenario 2 until the earthquake reaches a  $M_w$  3.5 where damage occurs in approximately 4% of the ground motions. For  $M_w$  5.5 and above at a distance  $R$  of 3 km the defined damage state is reached in 100% of the motions.

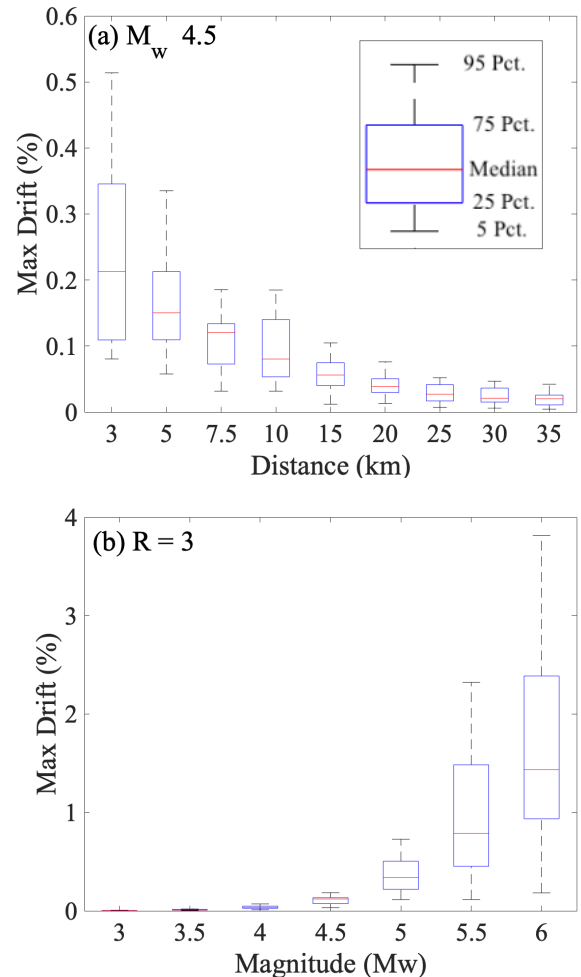


Figure 6: MDR from all simulations for (a) Scenario Set 1 and (b) for Scenario Set 2.

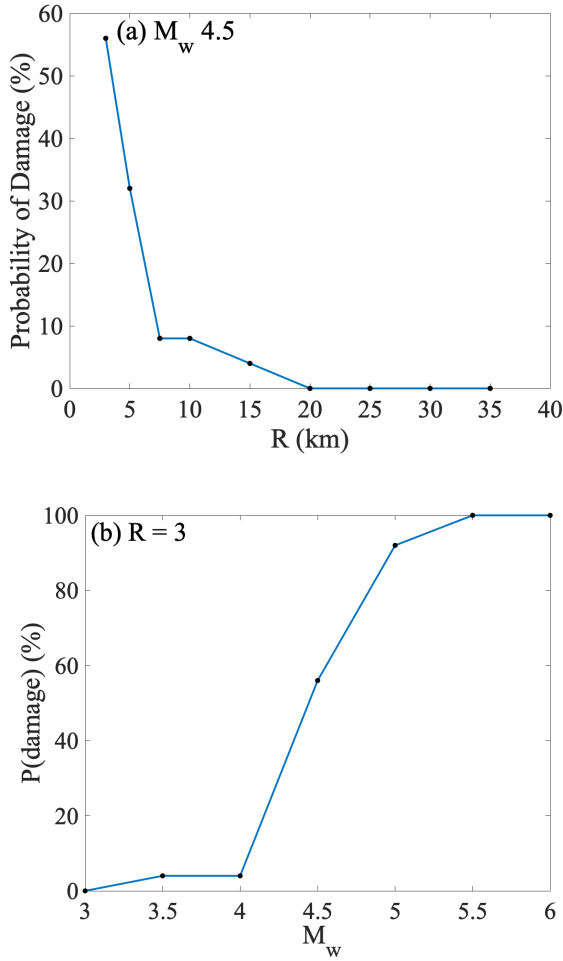


Figure 7: Percent of buildings reaching the defined damage threshold (a) for Scenario Set 1 and (b) for Scenario Set 2.

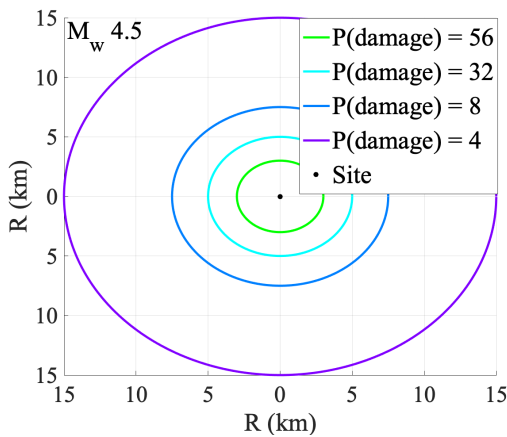


Figure 8: Geographical extent of damage for Scenario Set 1.

## 7. CONCLUSIONS

The purpose of this study is to determine what earthquake magnitudes at what distances can cause damage to a two-story multifamily light wood frame building that is designed for SDC B. First, we define a target spectrum using an OK-specific induced earthquake GMPE, and linearly scale induced ground motions to meet this target spectrum and spread. Then, we subject the building archetype modeled in Timber3D to the selected earthquakes to determine whether damage is observed. Damage is defined as 0.2% MDR.

The key findings of the study are as follows. First, the  $R$  threshold for damage to start appearing for Scenario Set 1 ( $M_w 4.5$ ) is an  $R$  of 15 km event, and the likelihood of damage increases as the earthquake gets closer. Second, the threshold for damage to start appearing for Scenario Set 2 ( $R$  of 3 km) event is a  $M_w 3.5$  event, and the damage is observed in all simulations for  $M_w 5.5$  events and above.

The building considered in this study is new construction that is designed to modern OK code standards. A majority of the existing building stock in OK is older than the considered building and lacks seismic detailing. As a result, this study potentially underestimates the likelihood of damage that would actually be observed for the postulated scenarios. Some future goals of this work are to examine a weaker building more typical of old OK building stock, to perform the analysis for multiple building types rather than just one multifamily dwelling, additional definitions of damage, and to continue the analysis for earthquakes ranging from  $M_w 3.0$  to  $M_w 6.0$  and distances ranging from  $R$  of 3 km to  $R$  of 260 km.

## 8. ACKNOWLEDGEMENTS

This research was supported by the National Science Foundation under award number 1520846 and by the Civil, Architectural, and Environmental Engineering at the University of Colorado, Boulder.

## 9. REFERENCES

- Applied Technology Council (ATC). (2012). "FEMA P58-1: Seismic Performance Assessment of Buildings - Methodology." 1(September), 278.
- ASCE. (2017). *ASCE 7-16. Minimum Design Loads for Buildings and Other Structures. American Society of Civil Engineers. Reston, VA. 2017.*
- Assatourians, K., Atkinson, G. M., and Assatourians, K. (2017). "Processed ground-motion records for induced earthquakes for use in engineering applications."
- Atkinson, G. M., and Assatourians, K. (2017). "Are Ground-Motion Models Derived from Natural Events Applicable to the Estimation of Expected Motions for Induced Earthquakes?" *Seismological Research Letters*, 88(2A), 430–441.
- Baker, J. W., and Lee, C. (2018). "An Improved Algorithm for Selecting Ground Motions to Match a Conditional Spectrum." *Journal of Earthquake Engineering*, 22(4), 708–723.
- Barba-Sevilla, M., Baird, B., Liel, A., Tiampo, K., Barba-Sevilla, M., Baird, B. W., Liel, A. B., and Tiampo, K. F. (2018). "Hazard Implications of the 2016 Mw 5.0 Cushing, OK Earthquake from a Joint Analysis of Damage and InSAR Data." *Remote Sensing*, 10(11), 1715.
- Briseghella, B., Demartino, C., Fiore, A., Nuti, C., Sulpizio, C., Vanzi, I., Lavorato, D., and Fiorentino, G. (2018). "Preliminary data and field observations of the 21st August 2017 Ischia earthquake." *Bulletin of Earthquake Engineering*, Springer Netherlands, (August 2017).
- Chase, R. E. (2018). "Structural Response and Risk Considering Regional Ground Motion Characteristics." University of Colorado at Boulder.
- Filiatrault, A., Fischer, D., Folz, B., and Uang, C.-M. (2002). "Seismic Testing of Two-Story Woodframe House: Influence of Wall Finish Materials." *Journal of Structural Engineering*, 128(10), 1337–1345.
- Ghehnavieh, E. Z. (2017). "Seismic analysis of light-frame wood building with a soft-story deficiency."
- Liu, T., Luco, N., and Liel, A. B. (2019). "Increases in Life-Safety Risks to Building Occupants from Induced Earthquakes in the Central United States." *Earthquake Spectra*, 35(3), 1–18.
- Novakovic, M., Atkinson, G. M., and Assatourians, K. (2018). "Empirically Calibrated Ground-Motion Prediction Equation for Oklahoma." *Bulletin of the Seismological Society of America*, 108(5A), 2444–2461.
- Pang, W., and Hassanzadeh Shirazi, S. M. (2013). "Corotational Model for Cyclic Analysis of Light-Frame Wood Shear Walls and Diaphragms." *Journal of Structural Engineering*, 139(8), 1303–1317.
- Petersen, M. D., Mueller, C. S., Moschetti, M. P., Hoover, S. M., Rukstales, K. S., McNamara, D. E., Williams, R. A., Shumway, A. M., Powers, P. M., Earle, P. S., Llenos, A. L., Michael, A. J., Rubinstein, J. L., Norbeck, J. H., and Cochran, E. S. (2018). "2018 One-Year Seismic Hazard Forecast for the Central and Eastern United States from Induced and Natural Earthquakes." *Seismological Research Letters*, 89(3), 1049–1061.
- Oklahoma Geologic Survey. (2018). "Oklahoma Earthquakes Magnitude 3.0 and greater."
- Weingarten, M., Ge, S., Godt, J. W., Bekins, B. A., and Rubinstein, J. L. (2015). "High-rate injection is associated with the increase in U.S. mid-continent seismicity." *Science*, 348(6241), 1336–1340.
- Yenier, E., and Atkinson, G. M. (2015). "Regionally Adjustable Generic Ground-Motion Prediction Equation Based on Equivalent Point-Source Simulations: Application to Central and Eastern North America." *Bulletin of the Seismological Society of America*, 105(4), 1989–2009.